JOURNAL OF MATERIALS SCIENCE **36** (2001) 1125–1131

Oxide ion conductivity in $La_{0.8}Sr_{0.2}Ga_{0.8}Mg_{0.2-x}Ni_xO_3$ perovskite oxide and application for the electrolyte of solid oxide fuel cells

T. ISHIHARA*, T. SHIBAYAMA, H. NISHIGUCHI, Y. TAKITA
Department of Applied Chemistry, Faculty of Engineering, Oita University,
Dannoharu 700, Oita 870-1192, Japan
E-mail: isihara@cc.oita-u.ac.jp

Although hole conduction was present, it was found that doping with Ni was effective in improving the oxide ion conductivity in $La_{0.8}Sr_{0.2}Ga_{0.8}Mg_{0.2}O_3$ based perovskite oxides. Considering the ionic transport number and the electrical conductivity, the optimized composition for Ni doped samples was $La_{0.8}Sr_{0.2}Ga_{0.8}Mg_{0.13}Ni_{0.07}O_3$ (LSGMN). In this composition, electrical conductivity was found to be virtually independent of the oxygen partial pressure from 1 to 10^{-21} atm. Consequently, the oxide ion conductivity was still dominant in this optimized composition. In agreement with the improved oxide ionic conductivity, the power density of the solid oxide fuel cell using $LaGaO_3$ as an electrolyte increased by doping with a small amount of Ni on the Ga site. In particular, the power density of 224 mW/cm^2 at 873 K, which is the maximum power density in the cells using $LaGaO_3$ based oxide as the electrolyte, was attained using LSGMN in spite of the use of electrolyte plates with a thickness of 0.5 mm. Therefore, LSGMN is highly attractive for the electrolyte material of low temperature operating SOFCs.

---

1. Introduction

Fuel cells are currently being developed as an environmentally concious electric power generating technology with almost no emissions of air pollutants and high efficiency for energy conversion. Therefore, development of a fuel cell system is also important for the suppression of CO_2 emissions. At present, the polymer electrolyte fuel cell (PEFC) is attracting much interest, since the low operating temperature makes the fabrication of the system easier and high power densities can also be attained. However, hydrogen in which the CO content is less than 10 ppm can only be used as the fuel. On the other hand, the solid oxide fuel cell, denoted as SOFC, is another type of interesting fuel cell from the power generation point of view since the energy conversion efficiency is particularly high and natural gas can be directly used as the fuel [1]. At present, Y_2O_3 stabilized-ZrO_2 (YSZ) is commonly used as the electrolyte in the solid oxide fuel cell (SOFC). As the oxide ion conductivity of YSZ is insufficient for the electrolyte of fuel cells, a thin electrolyte film without gas leakage and an excessively high operating temperature such as 1273 K are essential for achieving high power densities. However, the high operating temperature of the cell causes various difficulties which have to be overcome in order to obtain reliability as a power generator. All of the advantages of the SOFC such as high efficiency and a variety of fuel can be obtained at intermediate temperatures such as 1073 K. Furthermore, the choice of the materials for stacking cells becomes greater; in particular, cheap refractory metals such as stainless steel become usable by decreasing the operating temperature to 800 K. In addition, decreasing operating temperature is also effective in improving the start up and shut down characteristics of the cell. Consequently, a decrease in the operating temperature becomes highly important for the development of reliable and inexpensive SOFCs [2].

Decreasing the operating temperature requires a fast ion conducting electrolyte and an active electrode, in particular, the cathode [1]. In our previous study, it was found that a $LaGaO_3$-based perovskite type oxide exhibits high oxide ion conductivity [3, 4], which is comparable with that of CeO_2-based oxides. In particular, $LaGaO_3$ doped with Sr for La and Mg for Ga exhibits high oxide ion conductivity over a wide range of oxygen partial pressures. Following our reports, the high oxide ion conductivity of this system has been confirmed by several researchers [4–7]. One of the advantages of this oxide is that almost pure oxide ion conductivity is exhibited in both reducing and oxidizing atmospheres. It is reported that electron and/or hole

---

* Author to whom all correspondence should be addressed.

conduction in this oxide is smaller than that of the oxide ion by a few orders of magnitude [8]. It is, therefore, expected that the operating temperature of the SOFC can be decreased by using a $LaGaO_3$-based oxide as the electrolyte of the SOFC [9, 10]. High power density of the cell using a $LaGaO_3$ based oxide was also reported by several groups [11–14]. On the other hand, doping with transition metal cations is generally expected to be undesirable for an ionic conductor, since electronic conduction will increase. However, in our previous study, it was found that doping with Co is effective in improving the oxide ion conductivity when the amount of Co was less than 10 mol% on the Ga site [15]. In accordance with the improved oxide ion conductivity, the power density of the cell at intermediate temperatures was greatly improved by doping Co for Ga in $LaGaO_3$. It was also found that doping with Fe exhibited a positive effect on the electrical conductivity. In the present study, therefore, doping effects of Ni for Ga in $La_{0.8}Sr_{0.2}Ga_{0.8}Mg_{0.2}O_3$ on the oxide ion conductivity were studied. Furthermore, the power generation characteristics of the cell using Ni doped $LaGaO_3$ based oxide were investigated systematically.

2. Experimental

2.1. Preparation of $LaGaO_3$ based electrolytes doped with Ni

Calculated amounts of commercial La_2O_3 (Wako, 99.99% purity), $SrCO_3$ and MgO (Wako, 99.9% purity), Ga_2O_3 (Kishida, 99.99% purity), and NiO (99.5% Wako) were mixed in an Al_2O_3 mortar with a pestle and then precalcined at 1273 K for 6 h [7] to prepare perovskite oxides of composition $La_{0.8}Sr_{0.2}Ga_{0.8}Mg_{0.2-X}Ni_XO_3$. The resulting powders were pulverized and isostatically pressed into a disk (20 mm in diameter and 0.6 mm thickness) at 274.6 MPa in vacuum. The disks were sintered at 1773 K for 6 h. XRD measurement (Rigaku Rint 2500, Cu Kα radiation) was performed to analyze the purity of the specimens and it was confirmed that the specimens consisted of the single $LaGaO_3$ perovskite phase. SEM examination was performed with a Hitachi S-2400 (25 kV) to assess the microstructure of the obtained disk. Fig. 1 shows the SEM micorgraph obtained. It is clear that the obtained disk was highly dense and no significant open pores or holes were observed. The relative density, estimated using the Archimedes method, was always higher than 95% of the theoretical density. It is also noted that the primary grain size was distributed from 5 to 10 μm.

Disks were ground and polished with a diamond wheel to 0.5 mm in thickness. The electrolytes at this thickness were always used for the fabrication of the SOFC in this study.

2.2. Oxide ion conductivity and power generation characteristics measurement

The electrical conductivity was measured as a function of temperature and oxygen partial pressure by a conventional four-probe dc method in a gas flow. Each measurement was performed for a period longer than 1 h at each temperature and oxygen partial pressure in order to confirm a stable conductivity. The partial pressure of oxygen was controlled by mixing N_2, CO, or H_2 with O_2 and the oxygen partial pressure was monitored by a CaO stabilized ZrO_2 oxygen sensor that was attached close to the sample. The transport number of the oxide ion was estimated by the electromotive forces of the H_2-O_2 gas concentration cell. The oxygen partial pressure was adjusted by adding 3 vol% H_2O to H_2.

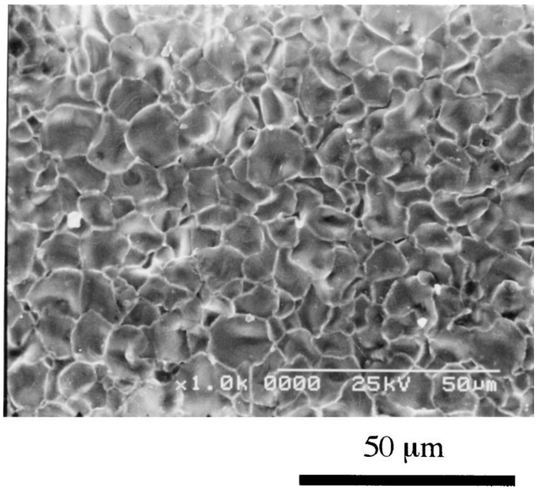

Figure 1 SEM micrograph of the resultant $La_{0.8}Sr_{0.2}Ga_{0.8}Mg_{0.13}Ni_{0.07}O_3$.

The commercial NiO (Wako, 99.9%) without further purification was used for the anodes. The prepared cathode oxide and the anode metal oxide were applied on the surface of the electrolyte by painting with *n*-butyl acetic acid solvent (5 mm in diameter). After drying at room temperature, the specimens were calcined at 1173 K for 10 min to remove the organic solvent. Before measurement of the power generation characteristics, NiO was reduced to Ni metal in a hydrogen stream at 1273 K. Molten Pyrex glass was used for sealing the cell. Commercial oxygen and hydrogen humidified with 3 vol% H_2O were used for the oxidant and the fuel, respectively, for the power generating measurements. It is also noted that the theoretical electromotive forces were 1.10 V.

3. Results and discussion

3.1. Effect of Ni doping for Ga site of $LaGaO_3$ on oxide ion conductivity

Fig. 2 shows the XRD patterns of Ni doped $La_{0.8}Sr_{0.2}Ga_{0.8}Mg_{0.2}O_3$ (LSGM). It is clear that the diffraction patterns from all specimens prepared in this study mainly consisted of those peaks attributable to the $LaGaO_3$ perovskite phase. Although no significant diffraction peaks from a secondary phase were observed, a weak peak was observed around 30 degrees on the sample at $X = 0.1$ in $La_{0.8}Sr_{0.2}Ga_{0.8}Mg_{0.2-X}Ni_XO_3$. This peak could be assigned to the $LaSrGaO_4$ phase. This $LaSrGaO_4$ phase easily forms on LSGM preparation. In addition, the diffraction peaks were shifted on doping with Ni. Therefore, it is considered that the doped Ni successfully substituted

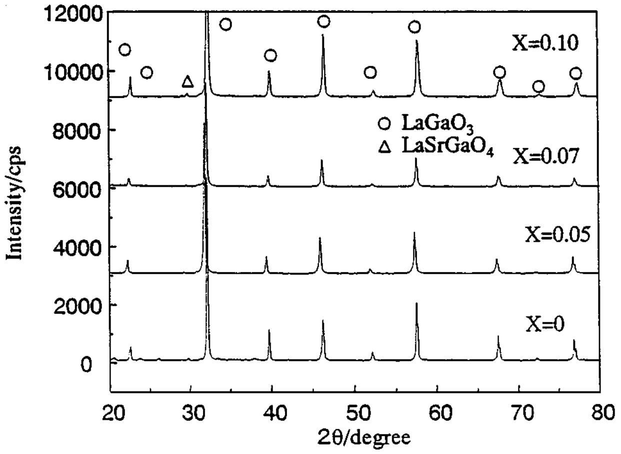

Figure 2 XRD patterns of Ni doped $La_{0.8}Sr_{0.2}Ga_{0.8}Mg_{0.2}O_3$.

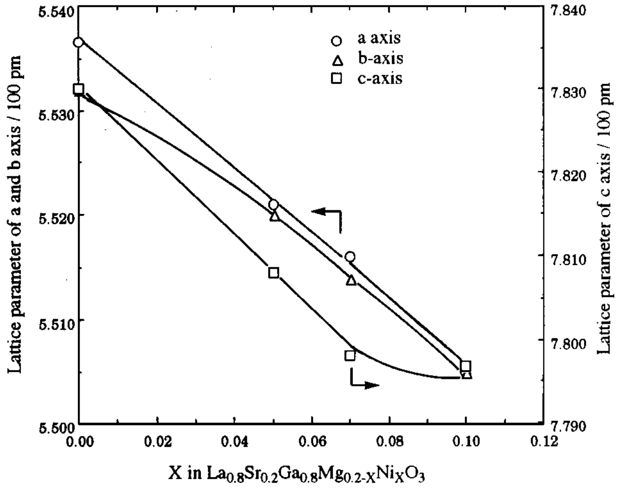

Figure 3 Estimated lattice parameter from XRD patterns as a function of Ni content.

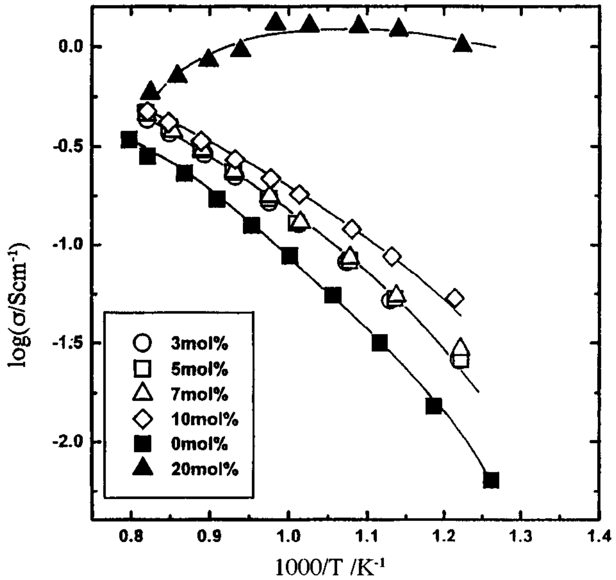

Figure 4 Arrhenius plots of the electrical conductivity of $La_{0.8}Sr_{0.2}Ga_{0.8}Mg_{0.2-X}Ni_XO_3$.

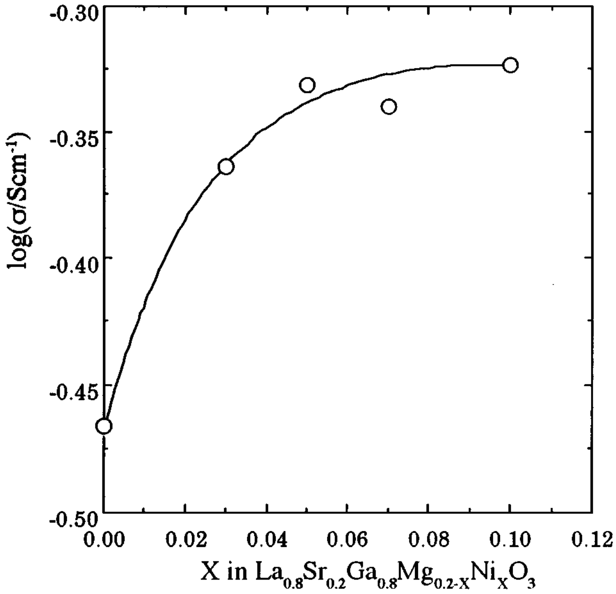

Figure 5 Electrical conductivity at 1123 K as a function of doped Ni amount.

for the Ga site in the $LaGaO_3$ lattice. The lattice parameters estimated with Rietveld method were shown in Fig. 3 as a function of Ni content. It is obvious that the lattice parameters of the *a*, *b*, and *c* axes decreased with increasing Ni content. Since the ionic size of six-coordinated Ni^{3+} (60 pm) is slightly smaller than that of Ga^{3+} (62 pm). Consequently, the shrinking unit lattice volume can be explained by the partial substitution of Ga^{3+} with Ni^{3+}. Although the divalent Ni is more stable under the conditions of this study, an abnormal valence number of trivalent Ni may be stable by substituting the trivalent cation of Ga in $LaGaO_3$ perovskite structure.

Fig. 4 shows the Arrhenius plots of the electrical conductivity of $La_{0.8}Sr_{0.2}Ga_{0.8}Mg_{0.2-X}Ni_XO_3$. In order to establish the optimum composition for the Ni dopant concentration, the total amount of dopant on the Ga site was fixed at 20 mol% to get the same oxygen deficiency as that in the parent LSGM provided that the doped Ni would take the divalent form. It is obvious that the electrical conductivity monotonously increased with increasing Ni content. At $X = 0.2$, conductivity changed from a semiconductor to a metallic behavior. This is quite similar to that of the Co doped sample. The electrical conductivity at 1123 K is shown in Fig. 5 as a function of doped Ni amount. It is clear that the electrical conductivity increased with increasing Ni concentration and it appears that it is independent of the Ni concentration for compositions where $X \geq 0.05$ in $La_{0.8}Sr_{0.2}Ga_{0.8}Mg_{0.2-X}Ni_XO_3$.

Fig. 6 shows the electrical conductivity of $LaGaO_3$ based oxide at 1173 K as a function of oxygen partial pressure. It is clear that the electrical conductivity was almost independent of the oxygen partial pressure in the range from $P_{O2} = 1$ to 10^{-21} atm when the Ni content was less than 10 mol% on the Ga site. Therefore, oxide ion conductivity was still dominant at this Ni content. In contrast, the electrical conductivity of the 20 mol% Ni doped sample decreased monotonously with decreasing oxygen partial pressure. Consequently, the major charge carrier at this composition seems to be the electronic hole. Therefore, in analogy with Co doping effects, doping with an excess amount of Ni only enhances the electronic hole conduction and is

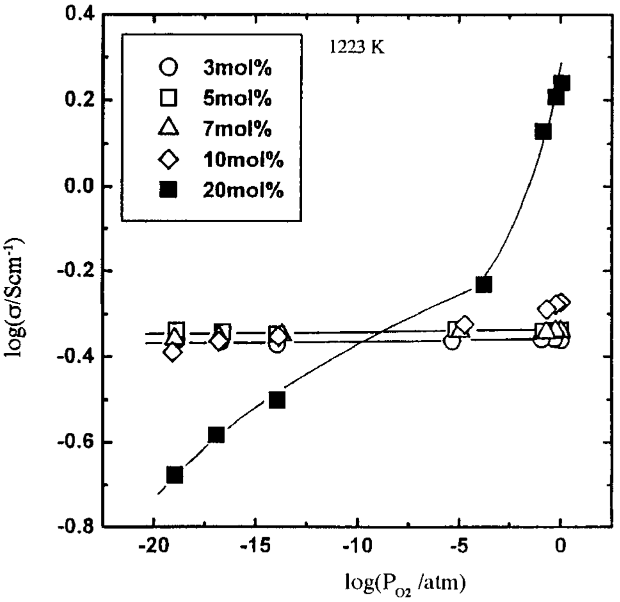

Figure 6 Electrical conductivity of $La_{0.8}Sr_{0.2}Ga_{0.8}Mg_{0.2-X}Ni_XO_3$ at 1173 K as a function of oxygen partial pressure.

undesirable for the pure oxide ion conductor. However, it is expected that doping with Ni at less than 10 mol% is effective for improving the oxide ion conductivity.

The transport number of the oxide ion in Ni doped $LaGaO_3$ based oxide was estimated with a H_2-O_2 gas concentration cell. Fig. 7 shows the temperature dependence of the transport number of the oxide ion which was estimated by the electromotive forces in a H_2-O_2 gas concentration cell. The transport number of the oxide ion decreased with decreasing temperature. Since it is well known that the activation energy for hole conduction is far smaller than that of oxide ion conduction, the electronic hole conduction became dominant with decreasing temperature. This was also confirmed by an increase in the P_{O2} dependence of the conductivity with decreasing temperature. On the other hand, in good agreement with the results in Fig. 6, it is obvious that the estimated transport number of the oxide ion decreased with increasing Ni content at the same temperature. However, the transport number of the oxide ion was still higher than 0.7 at all temperatures when the Ni content was less than 10 mol%. Therefore, it can be said that the oxide ion conductivity in $LaGaO_3$ based oxide increased by doping with a small amount of Ni on the Ga site. Since the electrical conductivity was almost independent of the oxygen partial pressure from $P_{O2} = 1$ to 10^{-21} atm, Ni doped $LaGaO_3$ exhibited stable oxide ion conductivity over a wide range of oxygen partial pressures. This Ni doping effect on the conductivity is quite similar to that of Co doping. Therefore, Ni doped $LaGaO_3$ could be used as an electrolyte for intermediate temperature SOFCs, which is similar to the Co doped one.

Fig. 8 shows the comparison of the oxide ion conductivity in Fe, Co, or Ni doped $LaGaO_3$ based oxide. It is clear that oxide ion conductivity increased by doping with either Fe, Co or Ni. Although the optimized amount for each dopant was different, the electrical conductivity of the sample at the optimized composition was almost the same, as shown in Fig. 8. The difference in the amount of optimized composition among Fe, Co, and Ni may be related to the ionic radius of each dopant. On the other hand, the estimated transport number of the oxide ion was high in Fe doped $LaGaO_3$ based oxide (close to unity). However, appearance of hole conduction became significant and so the ionic transport number decreased on doping with Ni or Co. This may be related to the stability of the valence number of the cation. This is because Fe^{3+} is more stable than either Co^{3+} or Ni^{3+}. In any case, $LaGaO_3$ based oxides doped with either Ni, Co, or Fe exhibit notably high oxide ion conductivity over a wide P_{O2} range.

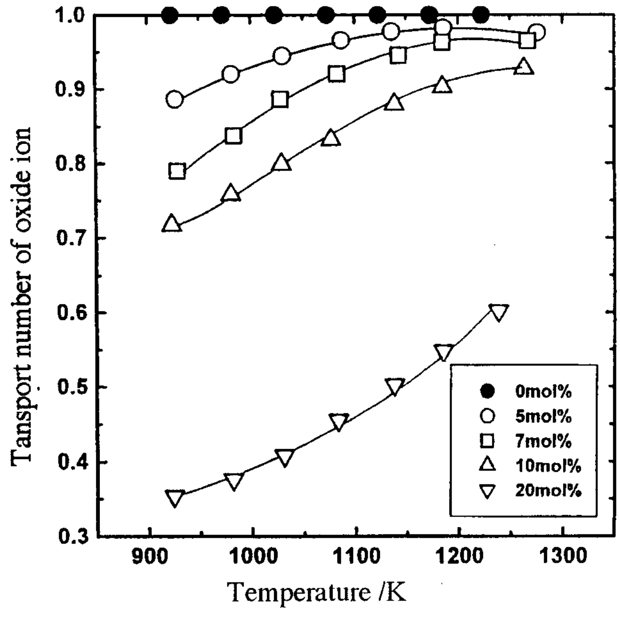

Figure 7 Temperature dependence of the transport number of oxide ions in $La_{0.8}Sr_{0.2}Ga_{0.8}Mg_{0.2-X}Ni_XO_3$.

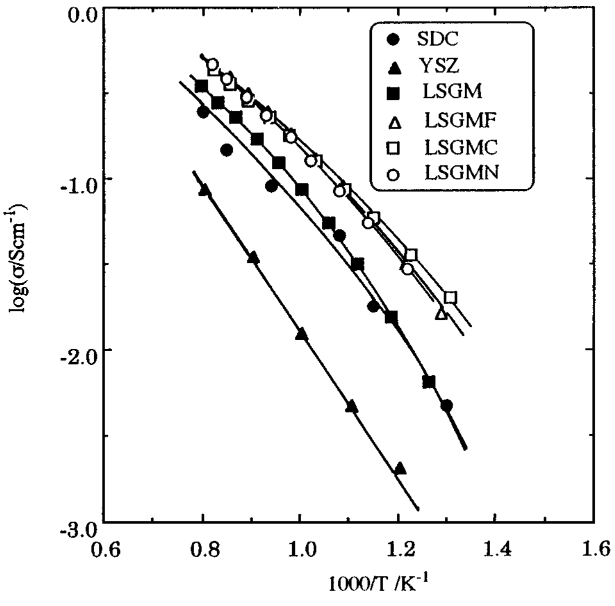

Figure 8 Comparison of the oxide ion conductivity in Fe, Co, or Ni doped $LaGaO_3$ based oxide. YSZ:$Zr_{0.86}Y_{0.14}O_2$, SDC:$Ce_{0.8}Sm_{0.2}O_2$, LSGM:$La_{0.8}Sr_{0.2}Ga_{0.8}Mg_{0.2}O_3$, LSGMF;$La_{0.8}Sr_{0.2}Ga_{0.8}Mg_{0.17}Fe_{0.03}O_3$, LSGMC;$La_{0.8}Sr_{0.2}Ga_{0.8}Mg_{0.115}Co_{0.085}O_3$, LSGMN; $La_{0.8}Sr_{0.2}Ga_{0.8}Mg_{0.13}Ni_{0.07}O_3$.

3.2. Electric power generation characteristic of SOFC using Ni doped $LaGaO_3$

The power generation characteristics of Ni doped $LaGaO_3$ were studied in detail. In order to determine the most suitable composition, the open circuit potential and the maximum power density of the cell at 1073 K is shown in Fig. 9 against the Ni content in $LaGaO_3$ based oxide. It is clear that the maximum power density increased with increasing Ni content and attained a maximum value at 7 mol% Ni doping on the Ga site of $LaGaO_3$. This dependence of maximum power density on Ni concentration is in good agreement with that of the electrical conductivity as shown in Fig. 3. For the composition of $La_{0.8}Sr_{0.2}Ga_{0.8}Mg_{0.13}Ni_{0.07}O_3$, the maximum power density was higher than 800 mW/cm^2 at 1073 K in spite of the use of a 0.5 mm thick electrolyte. On the other hand, the open circuit potential monotonously decreased with increasing Ni content. This is in good agreement with an increase in the hole conduction which was suggested by the electrical conductivity measurements. The improved power density also confirmed that the oxide ion conductivity improved by doping Ni for the Ga site. The optimized composition for the electrolyte of the SOFC seems to exist at $La_{0.8}Sr_{0.2}Ga_{0.8}Mg_{0.13}Ni_{0.07}O_3$ which is denoted as LSGMN in the following part.

Internal resistance of the cells which was estimated by the current interrupting method is shown in Fig. 10 as a function of Ni content. Clearly, the main internal resistance of the present cell was the electrical resistance (IR loss) which almost corresponded to that of the electrolyte. In agreement with the improved oxide ion conductivity, it is obvious that IR loss monotonously decreased with increasing Ni content. Therefore, the improved power density was a result of a decrease in IR loss. On the other hand, the cathodic overpotential of the present cell was quite small, since $Sm_{0.5}Sr_{0.5}CoO_3$ is highly active for the cathodic reaction at intermediate temperatures. In contrast, the anodic overpotential was much larger than that of the cathode. This suggests that the activity of pure Ni metal for the anodic reaction is not sufficient at intermediate temperatures. It is noted that the anodic overpotential decreased by doping Ni for $LaGaO_3$ electrolyte. At present, mechanisms for the decrease in anodic overpotential by doping Ni for the electrolyte are not clear. However, it is anticipated that the hole conduction produced by doping Ni for $LaGaO_3$ based oxide may have some relationship to the improvement of the anodic activity. Similar positive effects produced by electronic conduction in electrolytes on the electrode reaction were also reported on the cell using CeO_2 based oxide. In any case, it is obvious that the improved power density of the cell by using Ni doped $LaGaO_3$ based oxide for the electrolyte can be assigned to the decrease in IR loss. Consequently, it is considered that the power density will further increase by decreasing the thickness of the electrolyte. On the other hand, hole conduction was significant as an excess amount of Ni was doped on the Ga site and the cell was internally short-circuited. Therefore, although the IR loss monotonously decreased with increasing Ni content, the maximum power density decreased when the amount of Ni was in excess.

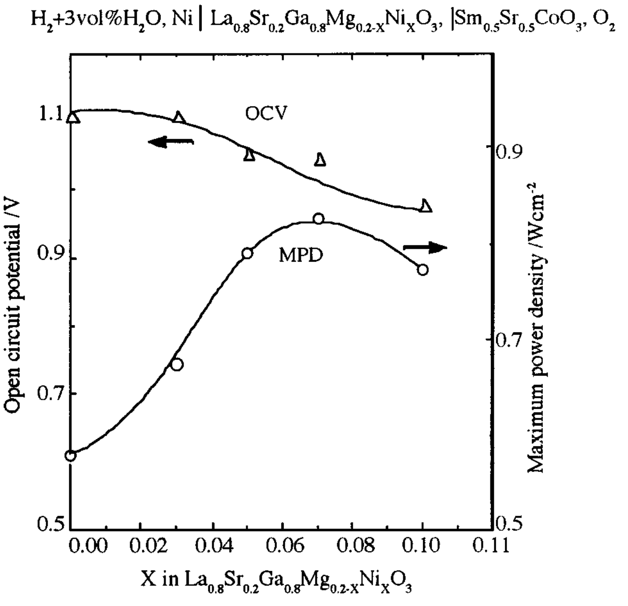

Figure 9 Open circuit potential (OCV) and the maximum power density (MPD) of the cell at 1073 K, which used Ni doped $LaGaO_3$ as an electrolyte.

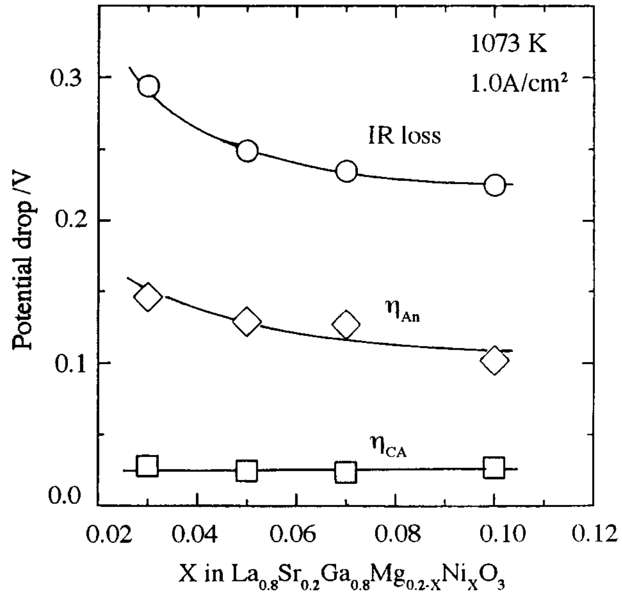

Figure 10 Internal resistance of the cells at 1073 K as a function of Ni content. IR loss; Ohmic loss, η_{CA}; Cathodic overpotential, η_{An}; Anodic overpotential.

Fig. 11 shows the temperature dependence of the maximum power density of the cell using LSGMN for the electrolyte. For the present cell, pure Ni is used as the anode. It is well known that Ni easily aggregates at a high current density and the power density decreases with the passage of time. Therefore, the power generation characteristic at temperatures higher than 1173 K was not measured in this study. It is obvious that the LSGMN cell exhibited a notably large power density and the high power density was sustained at low temperature. Although the thickness of the electrolyte used was as low as 0.5 mm, the maximum power density of the cell attained a value of 224 mW/cm^2 at 873 K, which was the largest power density attained in our previous

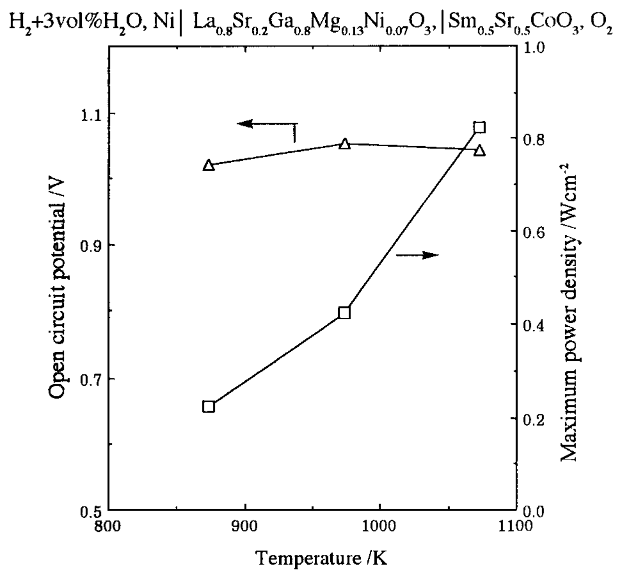

Figure 11 Temperature dependence of the maximum power density of the cell using LSGMN for the electrolyte.

study on the cell using $LaGaO_3$ based oxide as an electrolyte. The maximum power density of the cell with Y_2O_3-stabilized ZrO_2 electrolyte is 0.3 and 0.07 W/cm^2 at 1293 and 1073 K, respectively, when O_2 is used as oxidant. Considering the power density of the YSZ cell and the thickness of the electrolyte, the power density characteristics of the SOFC in Fig. 9 were extremely high. Since the ionic conductivity of YSZ at 1273 K is almost the same as that of LSGMN at 923 K, it is expected that equivalent performance would potentially be achieved at considerably lower temperatures. This, in our view, will be the most significant achievement in this field.

Fig. 12 shows the comparison of power generation characteristics of the cell utilizing the $LaGaO_3$ based oxide doped with Fe, Co, or Ni. The transport number of the oxide ion in non-doped and Fe doped $LaGaO_3$ is almost unity, however, that of Co or Ni doped specimens is slightly lower than 1 due to the hole conduction.

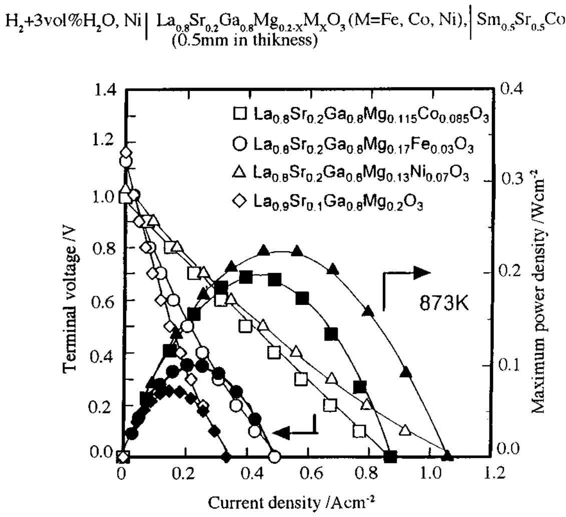

Figure 12 Comparison of power density of the cell utilizing the $LaGaO_3$ based oxide doped with Fe, Co, or Ni. Operating temperature was 873 K. Open symbol; I-V curve, Closed symbol; I-P curve.

In agreement with this result, the open circuit potential of the cells decreased in the following order of the electrolyte, non-doped > Fe ≫ Ni > Co doped $LaGaO_3$ as shown in Fig. 10. However, power density shows almost the opposite order and it increased in the following order, Ni > Co ≫ Fe > non-doped sample. It has been already reported that the maximum power density of the cell using Fe doped $LaGaO_3$ electrolyte exhibited a large power density at high temperature (0.7 W/cm^2 at 1073 K), however, it decreased drastically with decreasing temperature [16]. This may result from the large activation energy for the oxide ion conduction in Fe doped $LaGaO_3$. On the other hand, the Ni doped sample exhibited a similar performance to that of Co doped oxide, not only in the electrical conductivity but also in the electrical power generating characteristics when applied to the SOFC. Comparing with the internal resistance, the higher power density of the cell using Co, or Ni doped $LaGaO_3$ electrolyte rather than the Fe doped one may be assigned to a small overpotential of the electrode, in particular the anode. This may suggest that a charge transfer step is the rate-determining step for the electrode reaction and a little electronic conduction in the electrolyte could assist the charge transfer step resulting in a decrease in electrode overpotential. Consequently, overpotential of the electrode was reduced in the cell using Ni or Co doped $LaGaO_3$ based oxide electrolyte. Considering the power density and the open circuit potential, LSGMN seems to be more desirable as an electrolyte for intermediate temperature SOFCs.

4. Conclusions

Although hole conduction was observed at oxygen partial pressures higher than 10^{-5} atm, oxide ion conductivity increased by doping Ni for the Ga site of $LaGaO_3$. In accordance with the improved oxide ion conductivity, the power density of the cell also increased greatly by doping Ni for $LaGaO_3$ electrolyte. The highest power density in our previous study was attained with a cell using a $La_{0.8}Sr_{0.2}Ga_{0.8}Mg_{0.13}Ni_{0.07}O_3$ electrolyte. Since the valence number of Ni in the crystal lattice seems to be +2 or +3, it is anticipated that the number of oxygen vacancies was almost unchanged or decreased by doping with Ni. Consequently, the increased oxide ion conductivity may be assigned to improved mobility of the oxide ions. This is because the ionic size of six-coordinated Ni^{3+} is almost the same as that of Ga^{3+}. Any way, this study revealed that Ni doped $LaGaO_3$ based oxide was an attractive fast oxide ion conductor for the intermediate temperature solid oxide fuel cell. Since the notably high power density was exhibited at 873 K in spite of the use of 0.5 mm thick electrolyte, it is expected that the power density will further increase by decreasing the thickness of the electrolyte. This enables the operation of SOFCs at temperatures as low as 873 K, which may open a new application of the cell.

Acknowledgment

Part of this study was supported by Grant-in Aid from the Ministry of Education, Science, Culture, and Sports of Japan and the Nissan Research Foundation.

References

1. B. C. H. STEELE, *J. Power Source* **49** (1994) 1.
2. N. Q. MINH and T. TAKAHASHI, "Science and Technology of Ceramic Fuel Cells" (Elsevier, 1995).
3. T. ISHIHARA, H. MATSUDA and Y. TAKITA, *J. Am. Chem. Soc.* **116** (1994) 3801.
4. *Idem.*, *Solid State Ionics* **79** (1995) 147.
5. M. FENG and J. B. GOODENOUGH, *Eur. J. Solid State Inorg. Chem.* **31** (1994) 663.
6. P. N. HUANG and A. PETRIC, *J. Electrochem. Soc.* **143** (1996) 1644.
7. J. W. STEVENSON, T. R. ARMSTRONG, D. E. MCCREADY, L. R. PEDERSON and W. J. WEBER, *ibid.* **144** (1997) 3613.
8. R. T. BAKER, B. GHARBAGE and F. M. B. MARQUES, *ibid.* **144** (1997) 3130.
9. T. ISHIHARA, H. MINAMI, H. MATSUDA, H. NISHIGUCHI and Y. TAKITA, *Chemical Communications* (1996) 929.
10. T. ISHIHARA, M. HONDA, T. SHIBAYAMA, H. NISHIGUCHI and Y. TAKITA, *J. Electrochem. Soc.* **145** (1998) 3177.
11. R. MARIC, S. OHARA, T. FUKUI, H. YOSHIDA, M. NISHIMURA, T. INAGAKI and K. MIURA, *ibid.* **146** (1999) 2006.
12. M. FENG, J. B. GOODENOUGH, K. HUANG and C. MILIKEN, *J. Power Sources* **63** (1996) 47.
13. A. KHANDKAR, S. ELANGOVAN, A. HARTVIGSEN, D. ROWLEY, R. PRIVETTE and M. THARP, in Proc. of SOFC VI, edited by S. Signhal, M. Dokiya, and O. Yamamoto (1999) Vol. 99, 19, p. 88.
14. J. P. P. HUIJSMANS, F. P. F. VAN BERKEL and G. M. CHRISTIE, *J. Power Sorces* **71** (1998) 107.
15. T. ISHIHARA, T. AKBAY, H. FURUTANI, H. NISHIGUCHI and Y. TAKITA, *Solid State Ionics* **113–115** (1998) 583.
16. T. ISHIHARA, T. SHIBAYAMA, M. HONDA, H. NISHIGUCHI and Y. TAKITA, *Solid State Ionic Device, Electrochem. Soc. Proceeding Volume*, in press.

Received 2 May
and accepted 26 June 2000